

Charmed-particle production by photon-gluon fusion

L. M. Jones and H. W. Wyld

Department of Physics, University of Illinois at Urbana-Champaign, Urbana, Illinois 61801
(Received 25 July 1977)

We apply a simple extension of the gluon-fusion model of Einhorn and Ellis to the photoproduction of charmed particles at high energies. Overall rates of production are not much different from those predicted by various current models for strong production of charm, leading to the belief that charm should be more easily seen in the photoproduction case where backgrounds are smaller. The predictions of the model for various energy and angle distributions are presented. Predicted rates depend strongly on the mass of the charmed quark.

I. INTRODUCTION

A great deal of experimental effort is currently focused on the production of charmed particles in reactions other than e^+e^- annihilation. Various theoretical approaches applied to predictions of rates for these processes include both Okubo-Zweig-Iizuka (OZI)-rule-obeying and OZI-rule-violating processes. The OZI-rule-obeying processes [Fig. 1(a)] are generally rather severely suppressed¹ because of the expected low trajectories of the charmed exchanges and the large masses which must be produced. OZI-rule-violating processes can be calculated by introducing the gluons inherent in asymptotically free gauge theories. Two such processes are discussed in the current literature; these may be called the Drell-Yan process and gluon fusion. In the Drell-Yan process [Fig. 1(b)] a quark from one incident particle annihilates with an antiquark from the other incident particle to produce one or more gluons which then materialize in the form of charmed quarks (plus, of course, other quarks, gluons, etc. as required to conserve color and flavor quantum numbers).² In gluon fusion³ [Fig. 1(c)] the gluons from the two incident particles combine to produce the heavy charmed quarks.

The gluon-fusion mechanism has gained a great deal of support because it can be used to predict numbers for ψ production in hadronic experiments which are in reasonable agreement with the data.³ In this paper we point out that a trivial extension of this approach can be applied when one of the incident particles is a photon. Rates for charmed-particle production can be calculated which may be close to those recently detected at Fermilab. If one makes the additional assumption that the direction of the charmed quarks is maintained as that of the charmed particles after "dressing" has occurred, angular distributions for the inclusive production of charm can be computed.

In Sec. II we present the basic model together

with rates for production of charmed pairs computed for two currently fashionable gluon distribution functions. Angular distributions are discussed in Sec. III. Dependence on charmed-particle mass is discussed in Sec. IV.

II. MODEL

Our model is the process shown in Fig. 2. The gluon and incident photon "fuse" to form a charmed pair, which then is expected to clothe itself and shed its color with probability 1. By comparison

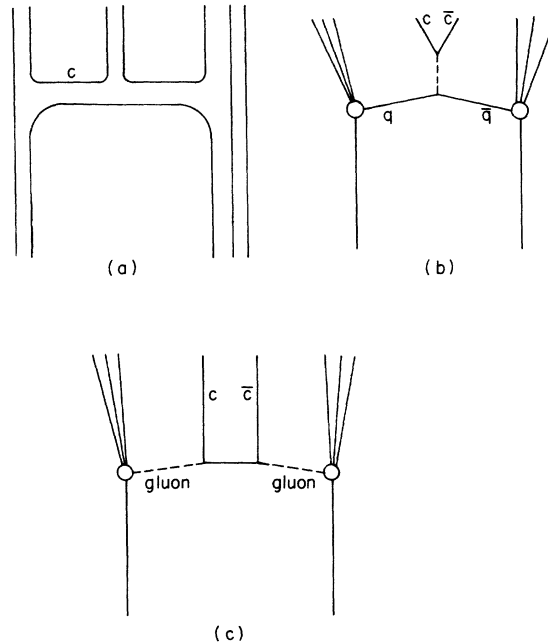


FIG. 1. Possible mechanisms for the production of charmed particles in hadronic processes: (a) An OZI-obeying process, containing exchange of a charmed trajectory. (b) A Drell-Yan process, based on annihilation of one quark from the beam particle with one quark from the target particle. (c) Gluon fusion.

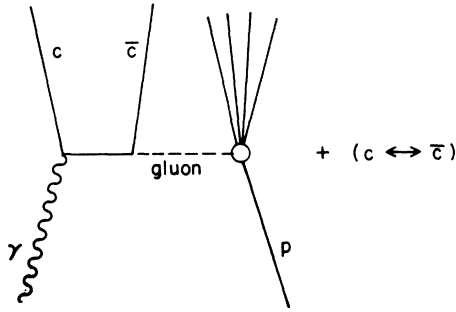


FIG. 2. Our model. The photon and gluon "fuse" to produce a pair of charmed quarks.

with the formula [their Eq. (7)] of Ellis and Einhorn³ for the process of Fig. 1(c), i.e.,

$$\left. \frac{d\alpha_{c\bar{c}}}{dM^2} \right|_{\text{Fig. 1(c)}} = \frac{\bar{\sigma}(M^2)}{s} \int_{M^2/s}^1 \frac{dx}{x} F(x) F\left(\frac{M^2}{sx}\right) \quad (1)$$

$$\sigma(M^2) = \frac{4\pi\alpha^2}{M^2} \left(\left(1 + 4 \frac{m_c^2}{M^2} - 8 \frac{m_c^4}{M^4} \right) \ln \left\{ \frac{M^2}{m_c^2} \frac{1}{2} \left[1 + \left(1 - 4 \frac{m_c^2}{M^2} \right)^{1/2} - 2 \frac{m_c^2}{M^2} \right] \right\} - \left(1 - 4 \frac{m_c^2}{M^2} \right)^{1/2} \left(1 + 4 \frac{m_c^2}{M^2} \right) \right) \\ \xrightarrow{m_c \ll M} \frac{4\pi\alpha^2}{M^2} \ln \frac{M^2}{m_c^2}. \quad (4)$$

All rates discussed here were calculated using a charmed-quark mass of $m_c = 1.65 \text{ GeV}$.⁴ The rates grow if the charmed-quark mass is decreased; this feature of the model is discussed in Sec. IV.

The form of gluon distribution functions is very uncertain at present. We follow Ellis and Einhorn³ in choosing

$$F(x) = \frac{1}{16} \frac{(n+1)}{x} (1-x)^n, \quad (5)$$

which is normalized so that the eight types of gluons together carry half the momentum of the target proton. We plot our results for the values $n=10$ and $n=5$. The value $n=10$ is the favored value obtained by Buras and Gaemers⁶ in recent fits to ep and μp deep-inelastic scattering data. The value $n=5$ is obtained from the counting rules.⁷

In Fig. 3 we display cross sections for production of charm, integrated over the mass M of the charmed pair, as a function of energy. We see that typical rates at low energy ($s = 200 \text{ GeV}^2$) are $0.25 \times 10^{-3} \text{ mb}$; at high energy larger rates such as $0.7 \times 10^{-3} \text{ mb}$ might be expected. These rates are similar to the rates obtained by Ellis and Einhorn³ for gluon fusion into charm in the *strong* interactions, at Fermilab energies ($s = 600 \text{ GeV}^2$), and are considerably larger than those obtained by

[where $\bar{\sigma}$ is the cross section for gluon + gluon \rightarrow quark + antiquark, and $F(x)dx$ is the number of gluons with momentum fraction between x and $x+dx$ in an incident proton], we can write down our formula for Fig. 2,

$$\frac{d\alpha_{c\bar{c}}}{dM^2} = \frac{\bar{\sigma}(M^2)}{s} F\left(\frac{M^2}{s}\right), \quad (2)$$

since the photon acts like a gluon of momentum fraction 1. Here $\bar{\sigma}$ differs from σ only in factors derived from color, the charmed-quark charge, and the difference between the strong and electromagnetic coupling constants. Both can be related to the cross section σ for photon + photon \rightarrow quark + antiquark:

$$\bar{\sigma} = \left(\frac{16}{9} \frac{\alpha_{st}}{\alpha} \right) \sigma. \quad (3)$$

In our calculations we have used the value $\alpha_{st} = 0.25$.⁴ The function σ is well known from electromagnetic calculations⁵ and is given by

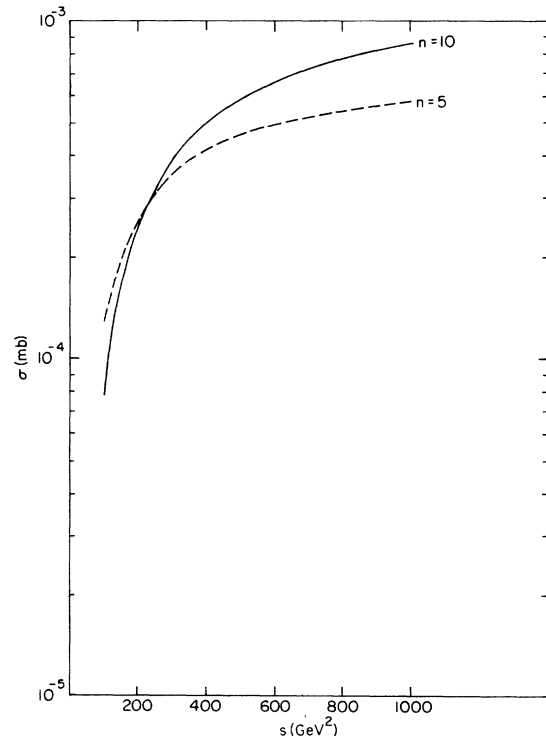


FIG. 3. Cross sections for the production of charm. n is the parameter in the gluon distribution function for the proton—see Eq. (5).

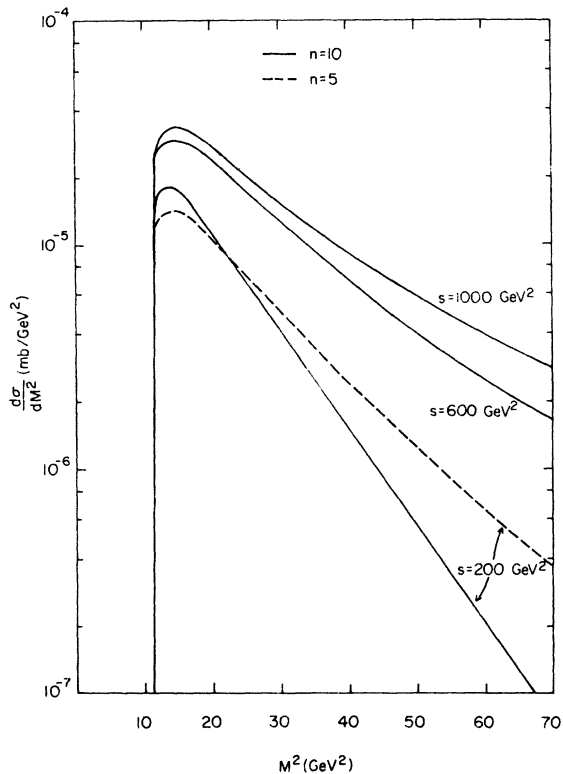


FIG. 4. Cross sections are peaked at low M^2 (the mass² of the charmed pair).

Fritzsch² for the same reactions and energies using a Drell-Yan mechanism.

Apparently the reduction in rate expected from using the electromagnetic coupling constant instead of the strong-coupling constant is more than compensated by not smearing over a distribution function $F(x)$ at the photon end. Since the backgrounds in strong interactions are much larger than in the photoproduction case, we expect the charm production to be much more visible in photoproduction. Indeed, at the time of this writing, charm has been reported in a photoproduction experiment at Fermilab⁸ and none has yet been seen in the hadronically induced reactions.

Equation (2) can also be used to predict the dependence of cross sections on the mass of the produced charmed pair; typical behavior is displayed in Fig. 4. There is a strong tendency to produce pairs of low mass.

III. ANGULAR DISTRIBUTIONS

In this sort of model, one is to imagine that the quarks seen as outgoing particles in Fig. 2 are

actually "clothed"—i.e., combined with additional quarks or antiquarks to make mesons or baryons—before they are observed. The clothing process is poorly understood, although work has been done by several authors⁹ to find clothing functions describing the materialization of particular quarks into particular mesons. We take the popular point of view that the charmed quarks *must* clothe themselves somehow (quark confinement), so that they clothe themselves with probability 1. Furthermore, we assume that they will prefer to clothe themselves with lighter quarks, so that our cross section for the production of charmed quarks will become exactly the total cross section for production of charmed mesons or baryons of all types. These assumptions allow us to believe that the cross sections displayed in Figs. 3 and 4 are representative of actual values for the production of pairs of charmed particles.

After we have made all these assumptions, it is natural to make the additional assumption that the quarks get dressed without changing their direction. This assumption is actually on much shakier ground than the ones previously discussed. However, there is some evidence¹⁰ in e^+e^- colliding-beam experiments that the produced hadrons come off in two jets, back to back in the center-of-mass system. This would coincide with the idea that the photon materialized into two quarks, which went off back to back in the center-of-mass system, and that these quarks then were clothed without changing direction. Our mechanism (Fig. 2) has the additional complication that the quark-antiquark pair is produced with color (since the incident particles are a colored gluon and an uncolored photon), and we must assume that this color leaks off somehow during the clothing process without changing the direction of the quarks. That is, we assume bremsstrahlung of wee gluons from the produced system in order for it to become colorless and hence observable. If we make all these assumptions, we can then use the angular distribution of the electromagnetic cross section to calculate the expected angular distribution of the charmed particles.

The theoretical development is very simple. We replace the total cross section $\bar{\sigma}(M^2)$ in Eq. (2) by the integral of a differential cross section and transform to appropriate variables. The differential cross section is given by Jauch and Rohrlich.⁵ Note that the gluon, projectile, and target masses are neglected (except for target mass terms necessary when transforming to the laboratory system). On the other hand, the charmed-quark mass is kept exactly. The invariant cross section for production of a charmed particle may be written in various ways:

$$\begin{aligned}
E \frac{d\sigma}{d^3p} &= \frac{s}{\pi} \frac{d\sigma}{dt dM_x^2} = \frac{4}{\pi s} \frac{d\sigma}{dx_1^2 dy} \\
&= \frac{1}{\pi s} \frac{1}{m_c^2 - t} F\left(\frac{M^2}{s}\right) M^4 \frac{d\hat{\sigma}(M^2, \hat{t}, \hat{a})}{d\hat{t}} \\
&= \frac{1}{\pi s^2} \frac{1}{x_2} F\left(\frac{x_2}{1-x_1}\right) M^4 \frac{d\hat{\sigma}(M^2, \hat{t}, \hat{a})}{d\hat{t}}, \quad (6)
\end{aligned}$$

where

$$\begin{aligned}
x_1 &= \frac{m_c^2 - u}{s} = \frac{1}{2}(x_1^2 + 4m_c^2/s)^{1/2} e^y, \\
x_2 &= \frac{m_c^2 - t}{s} = \frac{1}{2}(x_1^2 + 4m_c^2/s)^{1/2} e^{-y}. \quad (7)
\end{aligned}$$

Here $x_1 = 2p_{\perp}/\sqrt{s}$ and $y = \frac{1}{2}[\ln(E + p_{\parallel})/(E - p_{\parallel})]$ is the rapidity in the center-of-mass frame. The cross section for the subprocess gluon + photon \rightarrow quark + antiquark is given by

$$M^4 \frac{d\hat{\sigma}}{d\hat{t}} = \frac{16}{9} 4\pi \alpha \alpha_s X, \quad (8)$$

with

$$\begin{aligned}
X &= \frac{1}{2} \left(\frac{m_c^2 - \hat{t}}{m_c^2 - \hat{a}} + \frac{m_c^2 - \hat{a}}{m_c^2 - \hat{t}} \right) + 2 \left(\frac{m_c^2}{m_c^2 - \hat{t}} + \frac{m_c^2}{m_c^2 - \hat{a}} \right) \\
&\quad - 2 \left(\frac{m_c^2}{m_c^2 - \hat{t}} + \frac{m_c^2}{m_c^2 - \hat{a}} \right)^2 \\
&= \frac{1}{2} \frac{(1-x_1)^2 + x_1^2}{x_1(1-x_1)} + \frac{2m_c^2}{s} \frac{1}{x_1 x_2} \\
&\quad - 2 \left(\frac{m_c^2}{s} \right)^2 \frac{1}{(x_1 x_2)^2}, \quad (9)
\end{aligned}$$

where \hat{a} and \hat{t} are the momentum transfer variables for the subprocess. These kinematic variables are related by the following formulas:

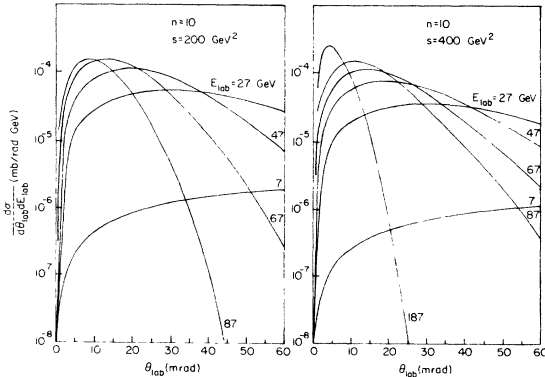


FIG. 5. Inclusive cross section for production of a charmed quark of the specified laboratory energy and angle.

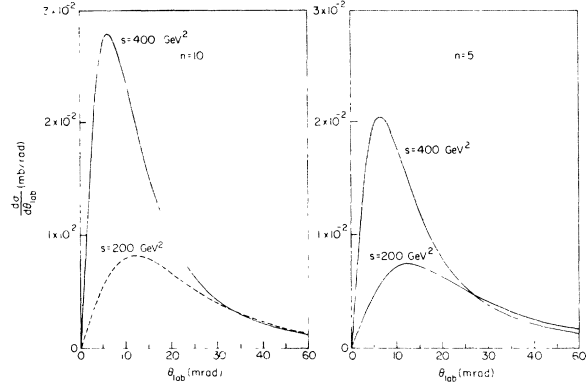


FIG. 6. Distributions integrated over energy peak much more sharply for larger s .

$$\begin{aligned}
s + t + u &= m_c^2 + M_x^2, \\
M^2 + \hat{t} + \hat{a} &= 2m_c^2, \\
\hat{t} &= t, \quad (10)
\end{aligned}$$

$$m_c^2 - \hat{a} = \frac{M^2}{s} (m_c^2 - u),$$

$$\frac{M^2}{s} = \frac{x_2}{1-x_1} = \frac{m_c^2 - t}{M_x^2 - t}.$$

These cross-section formulas are easily evaluated for any desired choice of variables. In view of experiments now underway at Fermilab we have calculated the distributions in laboratory energy E and laboratory angle θ :

$$\begin{aligned}
\frac{d\sigma}{d\theta dE} &= \frac{2 \sin \theta}{s} \frac{(E^2 - m_c^2)^{1/2}}{m_c^2 - t} F\left(\frac{M^2}{s}\right) M^4 \frac{d\hat{\sigma}}{d\hat{t}}, \\
m_c^2 - t &= \frac{s}{m_p} [E - (E^2 - m_c^2)^{1/2} \cos \theta], \quad (11)
\end{aligned}$$

$$M^2 = \frac{s(m_c^2 - t)}{s - 2m_p E},$$

where $m_p = 0.938$ GeV is the target mass. These are presented in Fig. 5 for the two energies $s = 200$ GeV² and $s = 400$ GeV² for the case where the parameter n in the gluon distribution is 10. Notice that particles with higher lab energies are produced with a much sharper angular distribution than those with lower lab energies. Note also that these figures are for the production of charm; multiply by 2 if it is irrelevant whether charm or anticharm is seen.

In Fig. 6 we present the results of integrating over lab energy to obtain angular behavior. The distribution peaks at very low angles in the lab (about 12.5 mrad for 200 GeV² and 7 mrad for 400 GeV²) and the peaks grow sharper with increasing energy. (In this range of energies the

overall cross section grows rapidly with energy, as shown in Fig. 3.) Notice that the behavior is qualitatively the same for the two values $n=5$ and 10 in the gluon distribution function.

IV. DEPENDENCE ON THE QUARK MASS

Our choice of 1.65 GeV for the quark mass is motivated by the work of De Rújula, Georgi, and Glashow;⁴ we decided to vary this parameter and were somewhat surprised to discover the sensitivity of the model to it. Total cross sections change over an order of magnitude between a quark mass of 1.65 GeV and one of 0.6 GeV (see Fig. 7). This is due to two effects:

- (i) At a given M^2 the cross section for the elementary process has some dependence on the quark mass—see Eq. (4).
- (ii) For low quark masses, much lower values of M^2 are allowed by kinematics. Since all the distributions peak at low M^2 , the additional area added from the low M^2 portion can be considerable.

Both effects are demonstrated in Fig. 8.

We have computed the curves in Figs. 7 and 8

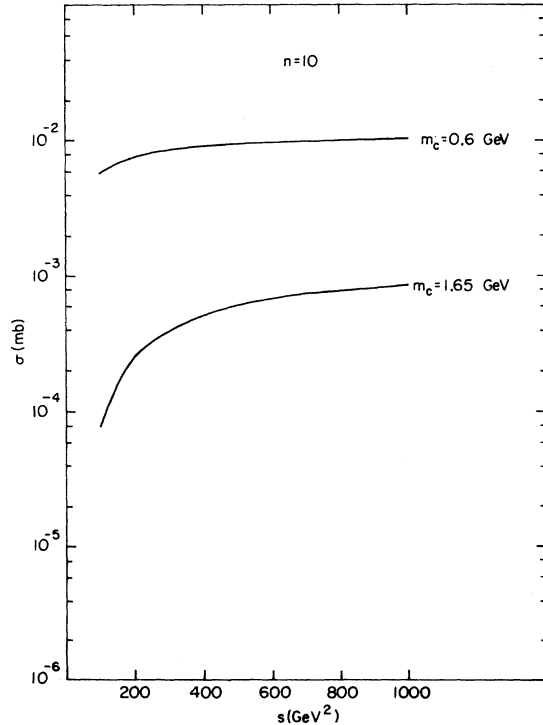


FIG. 7. Cross sections vary rapidly with the mass of the charmed quark. These curves are calculated for a quark of charge $\frac{2}{3}$. If one wishes to interpret the curve for $m_c = 0.6$ GeV as production of a strange $q\bar{q}$ pair, the values given should be divided by 4.

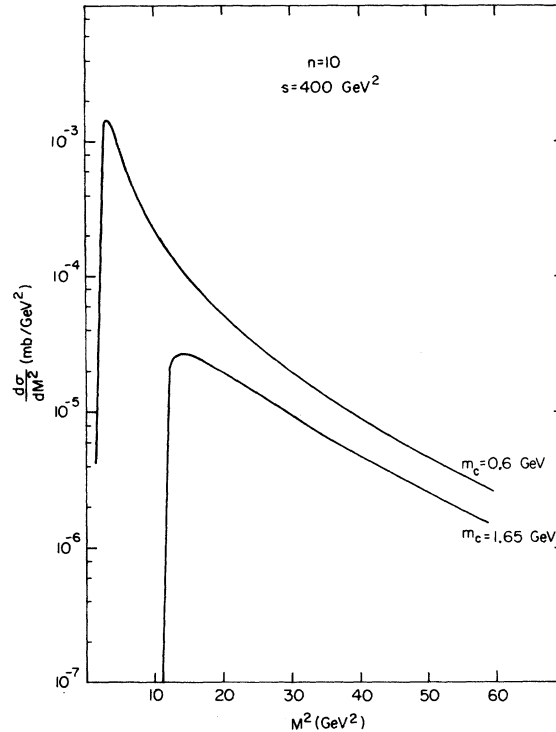


FIG. 8. Distributions in M^2 for different quark masses show that much of the difference in integrated cross section (Fig. 7) comes from the additional phase space at low M^2 for the low quark mass.

for a quark mass of 0.6 GeV with the idea that this should be a conservative estimate of the mass of the strange quark, and hence these curves should be underestimates of the amount of strange particles produced by this process in photoproduction. Presumably there are additional mechanisms for the production of strange particles, since the proton has a sea of strange-antistrange pairs which can be excited onto the mass shell. Hence one check on the validity of the model is provided by the curves marked $m_c = 0.6$ GeV in Figs. 7 and 8—they should be underestimates of the strange-particle production for incident photons.

V. SUMMARY AND CONCLUSIONS

We have applied the gluon-fusion approach to the production of charm by photon-gluon fusion. The resulting formula has several interesting features: (1) The photoproduction cross sections are comparable in magnitude to the strong-production cross sections—perhaps this accounts for the greater ease so far in finding charmed particles in the photon-induced process; (2) the numerical values depend rather strongly on the assumed charmed-quark mass—in addition to its experimental im-

plications this should be a warning to parton-model theorists who tend to set all masses equal to zero.

If the model is taken very seriously, and two further assumptions made (that the quarks clothe themselves without changing direction, and that color leaks away without affecting the direction of the quarks), detailed angular distributions can be predicted. These predictions are, of course, subject to assumptions about the form of the distribution of gluons in the proton; however, Figs. 3, 4, and 6 show that the main conclusions are similar for n of 5 and 10.

Note added. After this paper was completed, we received a report by Margolis¹¹ discussing a calculation of charm photoproduction in the standard vector-dominance model. He estimates contributions from the process in which the photon changes to a J/ψ , which then scatters diffractively off the nucleon; the diffractive scattering may dissociate the ψ into a charmed pair. His values for the contribution of charmed final states to the total γp cross section range from 2.3 to 5 μb , numbers somewhat larger than those displayed in Fig. 3. Both his estimate and ours are, of course, very dependent on the values inserted for various coupling constants, and we feel the two methods of

estimation are actually remarkably close. In fact, the calculations may be "dual" to each other in the following imprecise sense: The $c\bar{c}$ final state in our calculation must emit a gluon in order to become uncolored before its final clothing. This gluon will combine with the colored spray shown in Fig. 2 at the proton vertex to form colorless outgoing particles. Hence if one puts in all of the rearrangements in the final state, one has a diagram with two-gluon exchange with many of the characteristics of Pomeron exchange. In the Margolis technique, experiments on ψ photoproduction are used as input to a model with all of these final-state rearrangements included; in our technique the main input (values of α_{strong} and normalization of the gluon distribution function) is obtained from experiments on e^+e^- annihilation and inelastic electron scattering, and the final state is assumed to take care of itself. Clearly both approaches are approximations to some exact calculation in quantum chromodynamics; we hope experiments will soon determine whether either approximation is a good one.

This work was supported in part by NSF Grant No. PHY75-21590.

¹V. Barger and R. J. N. Phillips, Phys. Rev. D **12**, 2623 (1975); R. D. Field and C. Quigg, Fermilab Report No. 75/15-THY (unpublished).

²H. Fritzsche, Phys. Lett. **67B**, 217 (1977); Y. Kinoshita and K. Kinoshita, University of Bielefeld Report No. BI-TP 77/11 (unpublished).

³M. B. Einhorn and S. D. Ellis, Phys. Rev. D **12**, 2007 (1975); C. E. Carlson and R. Suaya, *ibid.* **14**, 3115 (1976).

⁴See for example T. Appelquist and H. D. Politzer, Phys. Rev. Lett. **34**, 43 (1975); Phys. Rev. D **12**, 1404 (1975); A. De Rújula, H. Georgi, and S. L. Glashow, *ibid.* **12**, 147 (1975); P. W. Johnson and W. K. Tung, Nucl. Phys. **B121**, 270 (1977); A. De Rújula, H. Georgi, and H. D. Politzer, Ann. Phys. (N.Y.) **103**, 315 (1977).

⁵J. M. Jauch and F. Rohrlich, *The Theory of Photons*

and Electrons (Addison-Wesley, Cambridge, Mass., 1955), p. 299.

⁶A. J. Buras and K. J. F. Gaemers, CERN Report No. TH.2322 (unpublished).

⁷S. J. Brodsky and G. Farrar, Phys. Rev. Lett. **31**, 1153 (1973); Phys. Rev. D **11**, 1309 (1975); R. Blankenbecler and S. J. Brodsky, *ibid.* **10**, 2973 (1974).

⁸B. Knapp *et al.*, Phys. Rev. Lett. **37**, 882 (1976).

⁹See for example D. Sivers, S. J. Brodsky, and R. Blankenbecler, Phys. Rep. **23C**, 1 (1976); L. M. Sehgal and P. M. Zerwas, Phys. Rev. Lett. **36**, 399 (1976); R. D. Field and R. P. Feynman, Phys. Rev. D **15**, 2590 (1977).

¹⁰G. G. Hanson *et al.*, Phys. Rev. Lett. **35**, 1609 (1975).

¹¹B. Margolis, Phys. Rev. D (to be published).